Neuron, Vol. 15, 1041–1051, November, 1995, Copyright © 1995 by Cell Press

huckebein Specifies Aspects of CNS Precursor Identity Required for Motoneuron Axon Pathfinding

Q. Chu-LaGraff,* A. Schmid,* J. Leidel,* G. Brönner,†‡ H. Jäckle,† and C. Q. Doe*
*Howard Hughes Medical Institute
Department of Cell and Structural Biology
University of Illinois
Urbana, Illinois 61801
†Max-Planck-Institut fur Biophysikalische Chemie
Abteilung Molekulare Entwicklungsbiologie
Postfac 2841
D-37018 Göttingen
Germany

Summary

***huckebein* encodes a putative zinc finger protein expressed in a subset of Drosophila CNS precursors, including the NB 4-2/GMC 4-2a/RP2 cell lineage. In *huckebein* mutant embryos, GMC 4-2a does not express the cell fate marker EVEN-SKIPPED; conversely, *huckebein* overexpression produces a duplicate EVEN-SKIPPED-positive GMC 4-2a. We use DiI to trace the entire NB 4-2 lineage in wild-type and *huckebein* mutant embryos. Loss of *huckebein* does not affect the number, position, or type of neurons in the NB 4-2 lineage; however, all motoneurons show axon pathfinding defects and never terminate at the correct muscle. Thus, *huckebein* regulates aspects of GMC and neuronal identity required for proper motoneuron axon pathfinding in the NB 4-2 lineage.**

Introduction

The question of how cell diversity is generated in the CNS is amenable to cellular, molecular, and genetic analyses in Drosophila. The CNS develops from neural precursors (neuroblasts; NBs) that divide asymmetrically to bud off smaller ganglion mother cells (GMCs). GMCs are intermediate precursors, dividing to produce two postmitotic neurons or glia. Each of the 30 NBs in a hemisegment can be uniquely identified based on its position, time of formation, and expression of molecular markers; most importantly, each NB generates a unique and reproducible clone of neurons and/or glia. Although the mechanisms governing NB formation are well understood (reviewed in Campos-Ortega, 1993), and progress has been made on how NB identity is determined (Chu-LaGraff and Doe, 1993; Zhang et al., 1994; Skeath et al., 1995), we know little about how cell diversity is generated within NB cell lineages.

To address the question of how cell fates are specified in the Drosophila CNS, we and others have focused on the NB 4-2 cell lineage. The first GMC born from NB 4-2 (GMC 4-2a) divides to produce the RP2 motoneuron and the RP2sib (Doe, 1992). A growing number of genes are known to be essential for the development of this early part of the NB 4-2 lineage. The *wingless* gene is required for specification of NB 4-2 and the activation of 5953, an enhancer-trap insertion expressed in NB 4-2 and the neuroectodermal cluster from which it delaminates (Chu-LaGraff and Doe, 1993). After NB 4-2 divides, GMC 4-2a expresses the genes encoding the homeodomain proteins PROSPERO (PROS), PDM-1, PDM-2, FUSHI TARAZU (FTZ), and EVEN-SKIPPED (EVE) (Doe et al., 1988a, 1988b, 1991; Yang et al., 1993; Bhat and Schedl, 1994). *pros*, *pdm-1*, *pdm-2*, and *ftz* are all required to activate *eve* expression in GMC 4-2a and its progeny, the RP2 and RP2sib. The loss of either *ftz* or *eve* CNS function often results in the transformation of the RP2 axon projection from ipsilateral to contralateral (Doe et al., 1988a, 1988b).

Although the NB 4-2 lineage is well characterized relative to other NB lineages, only a subset of the genes controlling the development of the NB 4-2 lineage has been identified. Genes acting between *wingless* in the neuroectoderm and *pros*, *pdm-1*, *pdm-2*, *ftz*, and *eve* expression in GMC 4-2a are currently unknown. The 5953 enhancer-trap insertion is activated in row 4 neuroectoderm and NB 4-2 in response to the *wingless* signal (Chu-LaGraff and Doe, 1993), and thus the associated gene is a prime candidate for a target of the *wingless* signal and a possible regulator of NB 4-2/GMC 4-2a cell fate. Our studies reveal that the 5953 enhancer trap is an insertion at the *huckebein* (*hkb*) locus. *hkb* encodes a putative zinc finger protein that is required for the repression of gap genes in the posterior embryonic region at the blastoderm stage (Brönner and Jäckle, 1991). During germ layer formation, *hkb* is required to specify endodermal cell fate by repressing ectodermal and mesodermal development in the endoderm primordia (Brönner et al., 1994; Reuter and Leptin, 1994).

In the developing CNS, *hkb* is expressed in NB 4-2 and GMC 4-2a, as well as in eight other NB lineages. We find that the loss of *hkb* results in a partial change in GMC 4-2a cell fate: there is a complete loss of *eve* expression, but *pros*, *pdm-1*, and *ftz* expression is normal. Conversely, overexpression of *hkb* produces a duplication of the EVE-positive GMC 4-2a and the RP2 neuron. To determine more precisely the role of *hkb* in the NB 4-2 lineage, we use the lipophilic fluorescent tracer DiI (Bossing and Technau, 1994) to reveal the complete embryonic cell lineage of NB 4-2 in wild-type and *hkb* mutant embryos. In embryos lacking *hkb* function, the NB 4-2 clone has the correct number and position of motoneurons and interneurons; however, motoneuron axon pathfinding is aberrant. In some cases, motoneurons reach their appropriate "muscle group," but never synapse with the correct muscle. Collectively, these results suggest that loss of *hkb* results in defects in GMC and neuronal fate leading to aberrant axon pathfinding.

‡Present address: Inst. für Neurophysiol., Univ. Köln, D-50931 Köln, Germany.

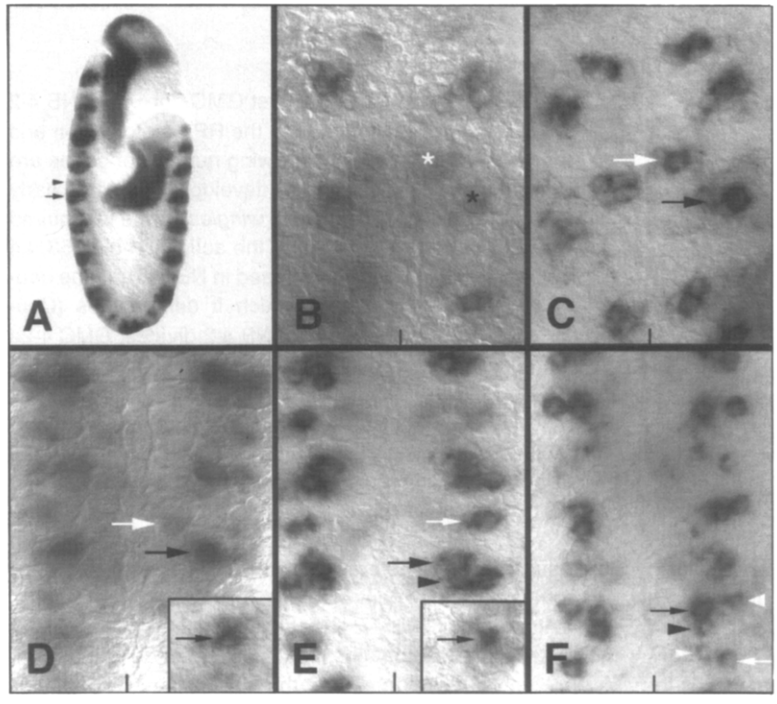

Figure 1. *hkb* Is Expressed in a Subset of Neuroectodermal Cells, Neuroblasts, and GMCs

Expression of hkb-lacZ (A) and *HKB* RNA (B–F) in wild-type embryos during early stage 9 (B), mid-stage 9 (C), stage 10 (D), stage 11 (A and E), and late stage 11 (F). Anterior is up; black line, ventral midline; (A), lateral view; (B–F), ventral view. NB stages and names are according to Doe, 1992, as modified by Broadus et al., 1995; embryo stages are according to Campos-Ortega and Hartenstein, 1985.

(A) Low magnification lateral view of a stage 11 embryo showing *hkb-lacZ* in a narrow band of neuroectodermal cells in row 2 (arrowhead) and in a large mediolateral cluster of neuroectodermal cells in rows 4 and 5 (arrow). *hkb-lacZ* is also transcribed in the anterior and posterior midgut primordia.

(B) Early stage 9 (S1 NB stage). *HKB* RNA is detected in neuroectodermal clusters at the positions where NBs 2-2 (white asterisk) and 4-2 (black asterisk) will delaminate.

(C) Mid-stage 9 (S2 NB stage). *HKB* RNA is expressed in NBs 2-2 (white arrow) and 4-2 (black arrow), and the neuroectodermal clusters at these positions.

(D) Stage 10 (S3 NB stage). *HKB* RNA is still expressed weakly in NB 2-2 (white arrow) and strongly in NB 4-2 (black arrow) and GMC 4-2a (inset).

(E) Early stage 11 (S4 NB stage). *HKB* RNA is expressed in NBs 2-4 (white arrow), 4-2 (black arrow), 5-4 (black arrowhead), and 1-1 and 4-4 (out of the focal plane). Neuroectodermal clusters at the 2-4 and 4-3/5-4 positions also express *hkb*. Inset, *hkb* expression in GMC 4-2a during early S4 (arrow); NB 4-2 is slightly out of focus and to the left of GMC 4-2a.

(F) Late stage 11 (S5 NB stage). *HKB* RNA is expressed in NBs 2-4 (white arrow), 4-3 (black arrow), 4-4 (large white arrowhead), 5-5 (black arrowhead), and 7-3 (small white arrowhead); there is no neuroectodermal expression. NB 4-2 has faint and variable expression at this stage; slightly later, *hkb* is not expressed in NB 4-2.

Results

Identification of the *huckebein* Gene

The 5953 enhancer-trap line was generated in a large-scale screen for lines with expression in a subset of NBs (Doe, 1992; C. Q. D. et al., unpublished data). We focused on 5953 because it is expressed in NB 4-2 in response to *wingless* (Chu-LaGraff and Doe, 1993). We find that the chromosome position, restriction map, and expression pattern of the transcription unit adjacent to the 5953 insertion match that of the *hkb* gene; moreover, 5953 imprecise excision mutations do not complement *hkb* alleles (data not shown). Thus, we refer to the 5953 pattern as *"hkb-lacZ"* and the adjacent gene as *hkb*.

hkb Is Expressed in a Subset of Neuroectodermal Cells, Neuroblasts, and GMCs

HKB RNA is expressed in a bisegmental pattern in the neuroectoderm (Figure 1). It is first detected in the CNS at early stage 9 in neuroectodermal clusters where NBs 2-2 and 4-2 will later form (Figure 1B); there is no expression in S1 NBs at this stage (Figure 2). At mid-stage 9, when the S2 NBs have formed, NBs 2-2 and 4-2 express *hkb* (Figure 1C). At stage 10 when the S3 NBs have formed, NB 2-2, NB 4-2, and GMC 4-2a express *hkb* (Figure 1D, inset); it is also expressed in a neuroectodermal cluster where NB 2-4 will delaminate and an expanded cluster where NBs 4-4 and 5-4 will delaminate (Figure 1D). Later in this stage, *hkb* is also faintly expressed in NB 1-1, which has already produced at least one GMC (data not shown). The expression in NB 1-1 midway through its cell lineage is different from all other *hkb*-expressing NBs, where *hkb* is expressed at the time of NB formation. At early stage 11 when the S4 NBs have formed, NBs 1-1, 2-4, 4-2, 4-4, and 5-4 express *hkb*, as do neuroectodermal clusters at the 2-4, 4-3, 5-4, and 7-3 positions (Figure 1E); *HKB* RNA is still detectable in GMC 4-2a (Figure 1E, inset). At late stage 11, when the S5 NBs have formed, NBs 1-1, 2-4, 4-2, 4-3, 4-4, 5-4, 5-5, and 7-3 all express *hkb* (Figure 1F). The first GMC born from NBs 2-4, 4-2, 4-3, 4-4, and 5-4 express *hkb* (data not shown). We have not determined whether other GMCs from these NBs express *hkb*, or whether other NBs produce *hkb*-positive GMCs. By the end of stage 13, all *hkb* CNS expression has disappeared except for a cluster of cells at a ventral/lateral position in every segment; by stage 15, *HKB* RNA is not expressed in the CNS.

The only detectable *HKB* RNA outside of the CNS is in the termini during blastoderm stage, anterior and posterior midgut primordia, and the salivary glands. In particular, *hkb* is not expressed in the PNS, trachea, mesoderm, lateral bodywall muscles, or lateral epidermis (tissues that could affect motoneuron axon pathfinding; see below).

Most NBs express *hkb* transiently at the beginning of

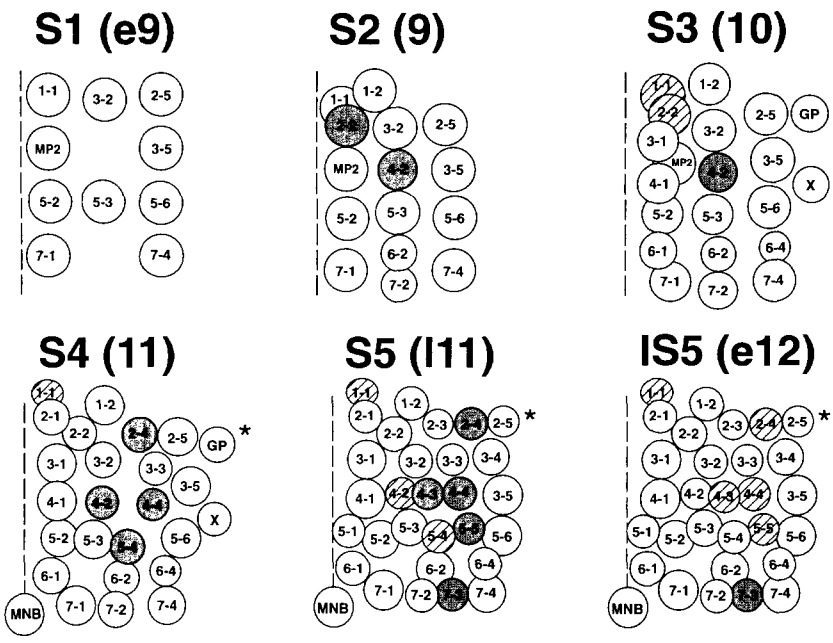

Figure 2. Summary of *hkb* Neuroblast Expression

Expression of *HKB* RNA in NBs. NB stages modified from Doe, 1992, according to Broadus et al., 1995; embryonic stages according to Campos-Ortega and Hartenstein, 1985, are indicated in parentheses. All NBs lack *hkb* expression by stage 13. Anterior is up; dashed line, ventral midline; asterisks, tracheal pits; dark gray, strong *hkb* expression; hatched, weak *hkb* expression.

their cell lineage, suggesting that *hkb* plays a role in the development of early-born GMCs. In this study, we examine the function of *hkb* in the NB 4-2 lineage, focusing on the firstborn GMC 4-2a and its RP2/RP2sib progeny. The function of *hkb* in other NB lineages will be described elsewhere (NBs 1-1 and 2-2: T. Bossing et al., unpublished data; NB 7-3: M. Lundell et al., unpublished data).

Loss of *hkb* Does Not Affect Neuroblast Formation or Markers for Neuroblast Identity

hkb is expressed in neuroectodermal clusters immediately prior to NB delamination; this is reminiscent of the expression pattern of proneural genes, which are required for NB formation (reviewed in Campos-Ortega, 1993). To determine whether *hkb* has a similar function, we examined NB formation in embryos homozygous for the strong hypomorphic allele hkb^{1} (hereafter called "*hkb* embryos"). We stained wild-type and *hkb* embryos for SNAIL (a marker for all newly formed NBs). *hkb* embryos have a normal pattern of NBs at all stages of neurogenesis (data not shown).

We tested for alterations in NB identity in *hkb* embryos using three molecular markers that are expressed in a subset of the *hkb*-positive NBs. The *runt* gene is expressed in NBs 1-1, 2-2, 2-5, 3-1, 3-2, 4-1, and 5-3 at stage 10 (Duffy et al., 1991; Chu-LaGraff and Doe, 1993); it overlaps with *hkb* in NB 1-1 and precedes it in NB 2-2. The *gooseberry-distal* gene is expressed in all row 5 and 6 NBs plus NB 7-1; it overlaps with *hkb* in NBs 5-4 and 5-5. The *seven-up-lacZ* (*svp-lacZ*) gene is expressed in all *hkb*-positive NBs (Doe, 1992; Broadus et al., 1995). A strong hypomorphic *hkb* allele (hkb^{62}; Q. C. -L. et al., unpublished data) was recombined onto the *svp-lacZ* chromosome to assay for alterations in the *svp-lacZ* pattern; the other markers were scored in an hkb^{1} background. For all three markers, NB expression pattern is the same in wild-type and *hkb* embryos (data not shown). Based on these three markers, there are no obvious alterations in NB identity in *hkb* embryos. Although these data do not rule out a role for *hkb* in specifying NB cell fate, they suggest that *hkb* may play a more subtle role in GMC and neuronal development. To investigate the CNS function of *hkb* in more detail, we focus on the NB 4-2 cell lineage.

hkb Is Required to Specify GMC 4-2a and RP2 Cell Fate

The first progeny of NB 4-2, GMC 4-2a, produces the identified RP2 motoneuron and the RP2sib and expresses *pros*, *pdm-1*, *pdm-2*, *ftz*, and *eve* (Doe et al., 1988a; Doe, 1992; Yang et al., 1993; Bhat and Schedl, 1994; Spana and Doe, 1995; Yeo et al., 1995). The *pros*, *pdm-1*, *pdm-2*, and *ftz* genes are required to activate *eve* expression, and both *ftz* and *eve* are required for normal axon pathfinding of the RP2 neuron (Doe et al., 1988a, 1991; Yang et al., 1993; Bhat and Schedl, 1994; Bhat et al., 1995; Yeo et al., 1995). In *hkb* embryos, we find no change in *pros*, *pdm-1*, or *ftz* expression in GMC 4-2a, but there is a complete loss of *eve* expression (Figure 3). The EVE-negative GMC 4-2a divides to produce an EVE-negative RP2 neuron and RP2sib (see below). These data show that *hkb* acts independently or downstream of *pros*, *pdm-1*, and *ftz* to activate *eve* expression in GMC 4-2a (Figure 3). We conclude that *hkb* is required for specifying at least one aspect of GMC 4-2a identity: the expression of *eve*.

hkb Overexpression Produces Duplicate EVE-Positive GMC 4-2a's and RP2 Neurons

To determine whether *hkb* is sufficient to generate the EVE-positive GMC 4-2a or RP2 cell fates, we overexpressed *hkb* at different stages of neurogenesis using an *hsp70-hkb* transgene ("*hs-hkb* embryos"; Brönner et al., 1994). As a control, we subjected *y w* embryos to identi-

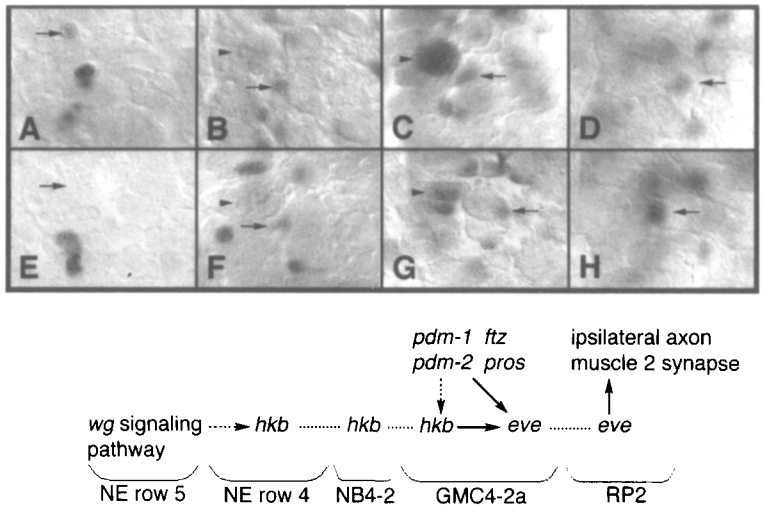

Figure 3. *hkb* Is Required for *eve* Expression in GMC 4-2a but Not for Expression of *pros*, *ftz*, or *pdm-1*

Wild-type embryos (A–D) and *hkb* embryos (E–H) labeled for EVE (A and E), PROS (B and F), FTZ (C and G), or PDM-1 (D and H) protein expression. Midline is at the left of each panel; anterior is up; black arrow, GMC 4-2a. In embryos stained for PROS (B and F) and FTZ (C and G), the MP2 precursor (arrowhead) was used as a landmark to help identify GMC 4-2a.

(A and E) EVE expression in stage 11 embryos. (A) Wild-type embryos have an EVE-positive GMC 4-2a. (E) *hkb* embryos lack the EVE-positive GMC 4-2a; this embryo is slightly older, and the two posterior clusters of EVE-positive cells have moved together.

(B and F) PROS expression stage 10 embryos. Both wild-type (B) and *hkb* (F) embryos have a normal PROS-positive GMC 4-2a.

(C and G) FTZ expression in stage 10 embryos. (C) Wild-type embryos have an FTZ-positive GMC 4-2a. (G) *hkb* embryos have a normal FTZ-positive GMC 4-2a; it is adjacent to NB 4-2 but slightly more lateral than in the wild-type hemisegment shown in (C).

(D and H) PDM-1 expression in stage 10 embryos. Both wild-type (D) and *hkb* (H) embryos have a normal PDM-1-positive GMC 4-2a.

(Diagram) The genetic hierarchy regulating *eve* expression in GMC 4-2a and the RP2 neuron. *wingless* (*wg*) activates expression of *hkb-lacZ* in row 4 neuroectodermal (NE) cells and is likely to activate *hkb* expression (dashed arrow). *hkb* is expressed in NB 4-2 and GMC 4-2a, where it activates *eve* but not *pros*, *ftz*, or *pdm-1* expression (arrow). *pros*, *ftz*, and *pdm-1/pdm-2* are required to activate *eve* expression in GMC 4-2a. *hkb* could be regulated by these genes (dashed arrow) or in a parallel pathway.

cal heat shock conditions. The most striking phenotypes are observed following *hkb* overexpression at stage 10, just after GMC 4-2a is born (Figure 4); overexpression of *hkb* at earlier or later times has little effect on GMC 4-2a fate (data not shown). Embryos were assayed at three timepoints: stage 11, when wild-type embryos have a single EVE-positive GMC 4-2a; stage 12, when wild-type embryos have a larger EVE-positive RP2 and smaller EVE-positive RP2sib; and stage 16, when wild-type embryos have a single EVE-positive RP2 neuron.

Heat-shocked *y w* embryos show a normal *eve* CNS pattern at all stages of development assayed (n = 198 hemisegments; Figures 4A–4C). In *hs-hkb* embryos assayed at stage 11, 19% of the hemisegments (n = 32) show two closely associated EVE-positive cells at the GMC 4-2a position (Figure 4D); these are likely to be the normal GMC 4-2a and a duplicate "GMC 4-2a." In *hs-hkb* embryos assayed at stage 12, 58% of the hemisegments (n = 76) show three or four EVE-positive cells at the RP2/RP2sib position (Figure 4E). In hemisegments with three EVE-positive cells, we observed two larger cells and one smaller cell; in hemisegments with four EVE-positive cells, we observed two larger and two smaller cells. The three-cell pattern is more common, but the exact proportions were not quantitated. In *hs-hkb* embryos assayed at stage 16, only 9% of the hemisegments contain a duplicate EVE-positive RP2 neuron (n = 120; Figure 4F). Our interpretation is that the duplicated GMC 4-2a fate is not completely stable. We conclude that *hkb* overexpression at stage 10 can generate a duplicate EVE-positive GMC 4-2a or RP2 neuron, probably by altering cell fates within the NB 4-2 lineage (see Discussion). Together, the loss-of-function and overexpression *hkb* phenotypes indicate that *hkb* plays a key role in the correct specification of GMC 4-2a identity (Figure 5).

RP2 Axon Pathfinding in *hkb*⁻ and *hkb* Overexpression Embryos

To characterize the role of *hkb* in the development of the GMC 4-2a/RP2 lineage in more detail, we stained *hkb* embryos for the axon markers BP102, fasciclin II, and fasciclin III (Patel et al., 1987; Grenningloh et al., 1991; Seeger et al., 1993). The overall structure of the CNS axon scaffold is normal, but there are occasional thin connectives and slightly fused commissures in some hemisegments (Figure 6). This may be due to interneuron axon pathfinding defects we observe in other NB lineages (e.g., the NB 1-1 and NB 2-2 lineages; T. Bossing et al., unpublished data).

To analyze the position and initial axon projection of RP2, we used the 22C10 antibody (Figure 7). 22C10 recognizes a membrane-associated epitope on a subset of neuronal cell bodies and axons (Fujita et al., 1982; Goodman et al., 1984). In wild-type embryos, the 22C10-positive, EVE-positive RP2 is located at the dorsal-most surface of the CNS at the junction of the anterior commissure and longitudinal connective; it projects in an anterior ipsilateral direction (Figure 7A) (Sink and Whitington, 1990). In *hkb* embryos, 70% of the hemisegments have an EVE-negative, 22C10-positive cell at the characteristic RP2 position (n = 66; the remaining hemisegments are EVE-negative but the 22C10 staining is ambiguous). Due to its close association with the 22C10-positive ventral unpaired median fascicle, it is difficult to determine the exact orientation of the "RP2" axon projection. In favorable preparations, we can observe either a posterior ipsilateral projec-

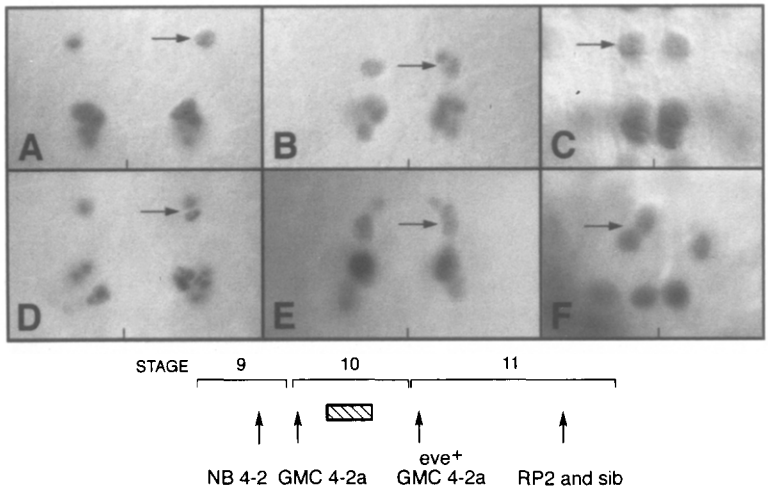

Figure 4. *hkb* Overexpression Results in Duplication of GMC 4-2a and RP2

y w embryos (A–C) and *y w; hs-hkb* embryos (D–F) were heat shocked at stage 10 and labeled for the EVE protein at stage 11 (A and D), 12 (B and E), or 16 (C and F). Anterior is up; black line, ventral midline. In all panels one segment is shown; (C) and (F) are at a higher magnification.

(A and D) Stage 11 embryos. (A) *y w* control embryos have one EVE-positive GMC 4-2a (arrow); (D) *hs-hkb* embryos have two EVE-positive cells at the GMC 4-2a position (arrow) in 19% of the hemisegments.

(B and E) Stage 12 embryos. (B) *y w* control embryos have a large EVE-positive RP2 and a small EVE-positive RP2sib (arrow). (E) *hs-hkb* embryos have three or four EVE-positive cells at this position in 58% of the hemisegments. The three-cell cluster has two large and one small cell (arrow); the four-cell cluster has two large and two small cells (not shown).

(C and F) Stage 16 embryos. (C) *y w* control embryos have a single EVE-positive RP2 neuron (arrow). (F) *hs-hkb* embryos have two EVE-positive "RP2" neurons (arrow) in 9% of the hemisegments.

(Diagram) Summary of the timeline for *hkb* overexpression. Embryos were heat shocked at stage 10 (hatched bar), just after GMC 4-2a is born (see Experimental Procedures for details).

tion (n = 4; Figure 7B) or an anterior ipsilateral projection (n = 4; data not shown); we never see a contralateral projection. The variable ipsilateral projection of the "RP2" neuron in *hkb* embryos is confirmed by DiI cell lineage analysis (see below).

As described in the previous section, overexpression of *hkb* produces a duplicate EVE-positive RP2 neuron in 9% of the hemisegments (see Figure 4). To determine whether this duplicate RP2 neuron has a normal axon projection, we stained *hs-hkb* embryos for EVE and 22C10 at stage 16. All duplicate EVE-positive RP2 neurons are also 22C10-positive; the normal and duplicate RP2s have tightly fasciculated axons projecting in the normal anterior ipsilateral direction (Figure 7C).

Together, the *hkb* loss-of-function and *hkb* overexpression results show that *hkb* is necessary to specify aspects of GMC 4-2a and RP2 cell fate (*eve* expression and a reliable anterior ipsilateral axon projection) and is sufficient to produce a duplicate GMC 4-2a/RP2 lineage.

DiI Tracing of the NB 4-2 Cell Lineage in Wild-Type Embryos

To obtain a more precise and comprehensive understanding of *hkb* function in the NB 4-2 lineage, we use the fluor-

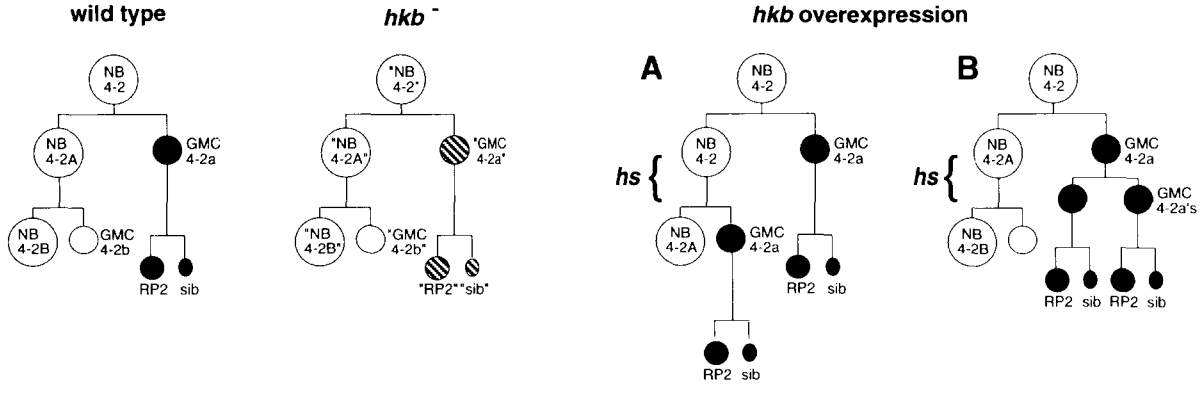

Figure 5. Models for the NB 4-2 Cell Lineage in *hkb* and *hkb* Overexpression Embryos

(Left) In wild-type embryos, GMC 4-2a expresses PROS, PDM-1, PDM-2, FTZ, and EVE (black); RP2 and the smaller RP2sib also express EVE (black).

(Middle) In *hkb* embryos, GMC 4-2a does not express EVE but still expresses PROS, PDM-1, and FTZ (hatched); it produces an EVE-negative RP2 neuron and RP2sib.

(Right) In embryos where *hkb* is overexpressed at stage 10 ("*hs*" bracket), just after GMC 4-2a is born, multiple EVE-positive cells are observed at the GMC 4-2a position. There are several interpretations for these results (see Discussion); the two most likely are (A) a transformation within the NB 4-2 lineage such that the second progeny (GMC 4-2b) adopts the fate of GMC 4-2a; and (B) an additional round of cell division in GMC 4-2a, resulting in the duplication of GMC 4-2a the subsequent duplication of RP2 and RP2sib.

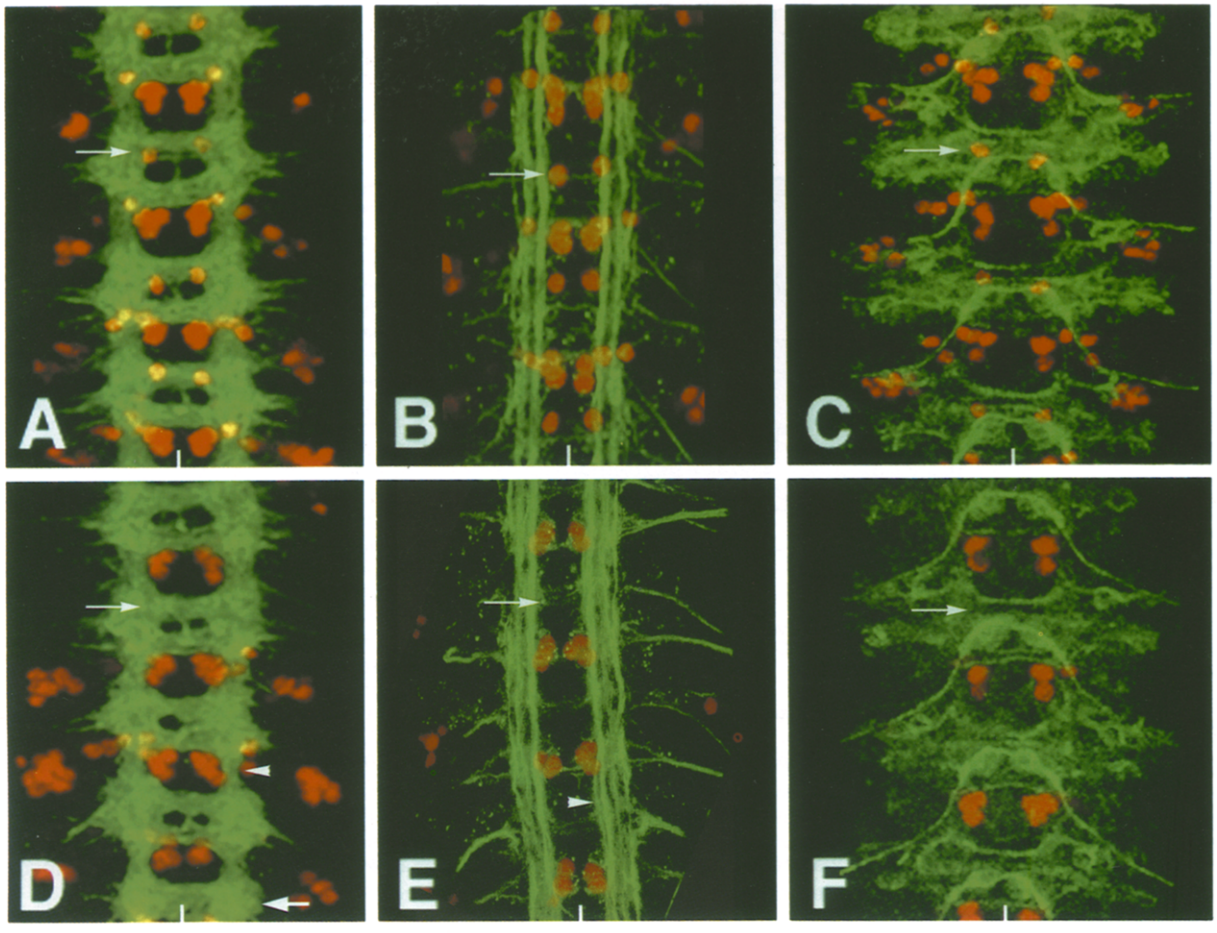

Figure 6. Organization of the CNS Axon Scaffold in *hkb* Embryos

Wild-type (A–C) and *hkb* (D–F) embryos double labeled for EVE protein (red) and BP102 (A and D), FAS II (B and E), or FAS III (C and F) axonal markers (green). Anterior is up; thin arrow, RP2 position; line, ventral midline.

(A and D) Stage 16 embryos stained for EVE and BP102. (A) Wild-type embryos show labeling of all longitudinal and commissural axons; there is a clear space between the anterior and posterior commissures. (D) *hkb* embryos have occasional thin connectives (arrowhead) or slightly fused commissures (thick arrow).

(B and E) Stage 16 embryos stained for EVE and FAS II. (B) Wild-type embryos have two well-defined longitudinal fascicles with continuous FAS II expression and a third more lateral fascicle with discontinuous expression. (E) *hkb* embryos show noticeable axon defasciculation in all fascicles.

(C and F) Stage 15 embryos stained for EVE and FAS III. (C) Wild-type embryos have five commissural fascicles labeled, three in the anterior commissure and two in the posterior commissure. (F) *hkb* embryos have a normal FAS III staining pattern.

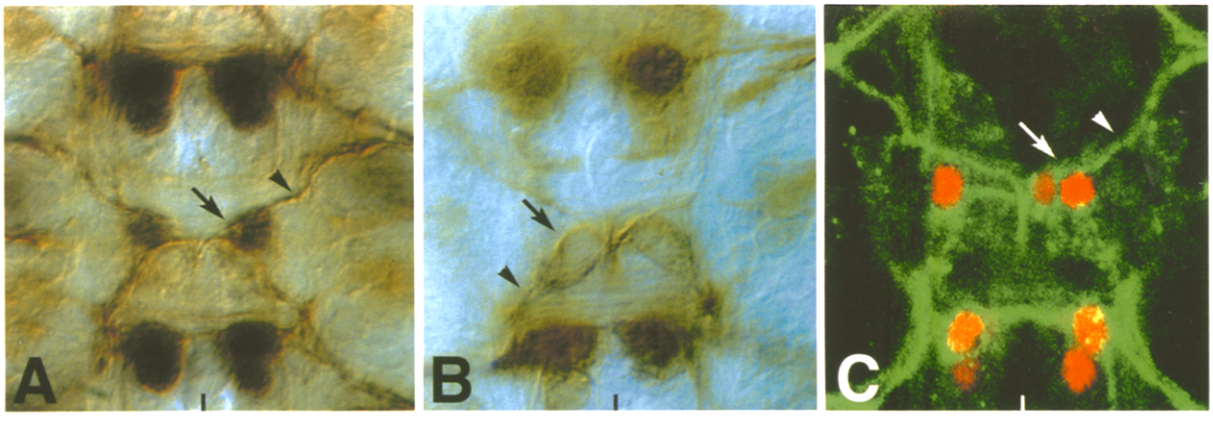

Figure 7. Axon Pathfinding of RP2 in *hkb* and *hkb* Overexpression Embryos

Stage 16 wild-type (A), *hkb* (B), and *hs-hkb* (C) embryos double labeled for the axonal marker 22C10 and EVE protein. In (A) and (B), EVE is in black and 22C10 is in orange; in (C), EVE is in red and 22C10 is in green. Anterior is up; line, ventral midline; arrow, RP2; arrowhead, putative RP2 axon.

(A) Wild-type embryo: RP2 is EVE-positive (black; arrow) and has a 22C10-positive axon (orange; arrowhead) projecting in an anterior ipsilateral direction (where it fasciculates with the 22C10-positive ventral unpaired median neurons).

(B) *hkb* embryo: a cell at the RP2 position is EVE-negative (arrow) and has a 22C10-positive axon (orange; arrowhead) projecting in a posterior ipsilateral direction. The "RP2" axon can also project in an anterior ipsilateral direction (not shown).

(C) *hs-hkb* embryo: two cells at the RP2 position are EVE-positive (red; arrow) and have 22C10-positive axons (green; arrowhead) projecting in an anterior ipsilateral direction (where they fasciculate with the 22C10-positive ventral unpaired median neurons).

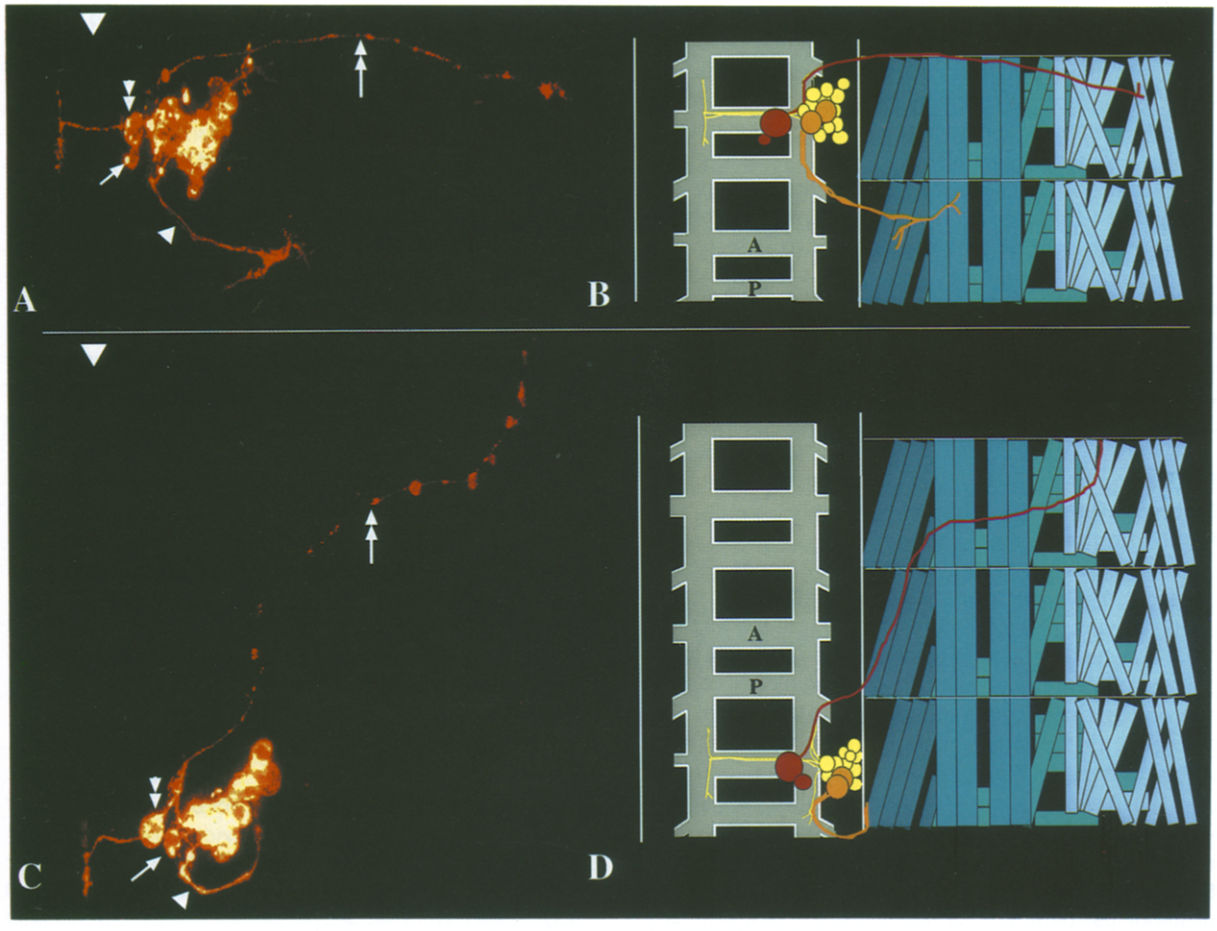

Figure 8. DiI Tracing of the Complete NB 4-2 Cell Lineage in Wild-Type and *hkb* Embryos

The NB 4-2 clone in stage 17 wild-type (A and B) and *hkb* (C and D) embryos. (A and C) Confocal images of DiI labeled NB 4-2 clones. The images are collected from living embryos, so some "blebbing" of cell membranes can occur; this does not affect axon trajectories. Anterior is up; large triangle, ventral midline; double arrowhead, RP2 cell body; double arrow, RP2 axon; arrow, putative RP2sib; small triangle, CoR axons. (B and D) Schematic drawings of the same clones. Outline of the CNS is in white with the neuropil in gray. RP2 and putative RP2sib, red; CoRs, orange; interneurons, yellow. Muscle groups are named according to Van Vactor et al., 1993: ventral, dark blue; ventral–lateral, medium dark blue; lateral, medium light blue; dorsal, light blue. Individual muscles are named according to Crossley, 1978. Axons project below the muscles (externally) but are shown above for clarity.

(A and B) Wild-type DiI-labeled NB 4-2 clone. The RP2 motoneuron has an anterior ipsilateral projection to muscle 2 in the dorsal muscle group; the small putative RP2sib is ventral to RP2 and has no axon; two CoR motoneurons have posterior ipsilateral projections to muscle 6 and muscle 16; and a cluster of 8–12 interneurons have projections across the anterior commissure with a bifurcated ending in the longitudinal connective.

(C and D) *hkb* DiI-labeled NB 4-2 clone. The NB 4-2 clone includes the same identified neurons as in wild type, but all motoneurons show abnormal axon pathfinding. The RP2 can wander across several segments and always terminates more ventrally than in wild type. (The axon shown has a putative synapse in the cleft between muscles 19 and 20; in the other three clones, the RP2 axons all terminate at the ventral side of the dorsal muscle group with no sign of a mature synapse.) The CoRs also show axon pathfinding errors (see text). In two clones, both CoR motoneurons terminate more ventrally than wild type. (One of these clones is shown; one other clone has identical CoR projections; and the other two clones have CoR axons that terminate near the middle of the ventral muscle group.) In all four clones, the CoR neurons show no sign of synapse formation. An independent NB clone in the adjacent anterior segment has been cropped out for clarity.

escent lipophilic tracer DiI (Bossing and Technau, 1994) to label NB 4-2 and its clone of neuronal progeny in wild-type and *hkb* embryos.

We generated nine wild-type NB 4-2 clones; we scored them as NB 4-2 clones because they contain the distinctive RP2 neuron. In both thoracic and abdominal segments, each clone reproducibly contains the following cells (from dorsal to ventral in the CNS). The RP2 motoneuron lies at the dorsal surface of the CNS above the junction of anterior commissure and longitudinal connective; it is displaced from the rest of the clone in a dorsal and medial direction (Figures 8A and 8B). The RP2 axon projects in an anterior ipsilateral direction into the intersegmental nerve and forms a mature synapse (bifurcated with close muscle contact) on muscle 2 in the dorsal muscle group (Figures 8A and 8B). The small putative RP2sib is located just ventral to RP2 and has no axon projection at mid-stage 17; it is also medially displaced from the rest of the clone (Figures 8A and 8B). A pair of motoneurons ("Cousins of RP2"; CoR) are tightly fasciculated and project posteriorly

and ipsilaterally out the intersegmental nerve root; one terminates at muscle 6 and the other terminates at muscle 16. Finally, there is a ventral cluster of 8–12 interneurons with axon projections contralateral in the anterior commissure; they bifurcate and terminate in the longitudinal connective (Figures 8A and 8B).

DiI lineage analysis shows that the entire wild-type embryonic NB 4-2 lineage contains the RP2 motoneuron, putative RP2sib, two CoR motoneurons, and a cluster of local commissural interneurons. Thus, NB 4-2 generates a clone with reproducible cell numbers, cell positions, cell types (interneuron/motoneuron), axon trajectories, and synaptic targets. There is variability in the number of interneurons (8–12), perhaps owing to differences in the age of the embryos.

DiI Tracing of the NB 4-2 Cell Lineage in *hkb* Embryos: Defects in Motoneuron Axon Pathfinding and Target Recognition

In *hkb* embryos, we generated five NB 4-2 clones (Figures 8C and 8D). We identified these as NB 4-2 clones based on the large number of features shared with the wild-type NB 4-2 clone. First, the RP2 motoneuron is dorsal to the junction of anterior commissure and longitudinal connective, and its axon projects ipsilaterally like the normal RP2. Moreover, it is the dorsal-most cell in the clone and is more medial and dorsal than the rest of the clone (Figures 8C and 8D). Second, there is a small putative RP2sib just ventral to the RP2 motoneuron; it has no projection and is medially displaced from the rest of the clone (Figures 8C and 8D). Third, there are two CoR motoneurons with posterior ipsilateral axon projections to the ventral muscle group (Figures 8C and 8D). Finally, there is a ventral cluster of interneurons that project contralaterally in the anterior commissure before bifurcating and terminating in the longitudinal connective (Figures 8C and 8D). The interneurons are identical to the wild-type NB 4-2 interneurons by all criteria assayed (number, position, and axon trajectory).

Despite the obvious similarity to the wild-type NB 4-2 clone, the NB 4-2 clone is clearly abnormal in *hkb* embryos. All motoneurons have axon pathfinding defects. In three of the four clones, the RP2 motoneuron projects anteriorly and ipsilaterally (like wild type), but in one case it projects posteriorly and ipsilaterally; however, in all four clones, the RP2 shows axon pathfinding defects once out of the CNS. For example, in one clone, it wanders anteriorly across several segments before terminating in the dorsal muscle group (Figures 8C and 8D). The CoR motoneurons also show axon pathfinding defects. In two of the four clones, the CoR axons leave their normal pathway on the external muscle surfaces (or never make contact) and reach the ventral epidermis before growing back into the embryo and terminating in the ventral muscle group (data not shown).

In addition to axon pathfinding errors, both RP2 and CoR neurons have possible target recognition defects and delayed/defective synapse formation (Figures 8C and 8D). In all four clones, RP2 reaches the dorsal muscle group but fails to contact its normal target, muscle 2. All RP2 neurons terminate at sites more ventral than normal (Figures 8C and 8D). Only one RP2 neuron has an ending that might be a mature synapse, showing extensive, close contact in the cleft between muscles 19 and 20 (Figure 8D); other RP2 neurons show no sign of synapse formation (e.g., a bifurcated ending or close contact with a muscle). The two CoR motoneurons also show possible target recognition defects (Figures 8C and 8D). In two clones, both CoR axons remain tightly fasciculated and terminate just beyond the edge of the CNS, at the ventral side of the ventral muscle group (Figures 8C and 8D). In the other two clones, the CoR axons defasciculate after reaching the periphery (as in wild type), but both endings appear to be ventral to their normal muscle targets. In all four clones, the CoR motoneurons show no sign of forming mature synapses.

The observation that an "NB 4-2" clone can be identified in *hkb* embryos by numerous criteria indicates that loss of *hkb* does not alter the fundamental identity of NB 4-2. In *hkb* embryos, NB 4-2 generates the correct number of interneurons and motoneurons at their normal positions. However, the RP2 and CoR motoneurons show frequent axon pathfinding errors and a delay or failure in establishing mature synapses.

Discussion

The Role of *hkb* in Specifying GMC 4-2a and RP2 Cell Fate

It is known that *pros*, *ftz*, *pdm-1*, and *pdm-2* are all expressed in GMC 4-2a and are required to activate *eve* expression. Here we show that *hkb* is also expressed in GMC 4-2a and is required for *eve* expression, but not for the expression of *pros*, *ftz*, and *pdm-1*. Thus, *hkb* acts downstream or in parallel to *pros*, *ftz*, and *pdm-1* in the genetic hierarchy leading to *eve* activation in GMC 4-2a (see Figure 3). It is not known what function, if any, each gene has in addition to triggering *eve* expression; it may be that each gene controls specific aspects of GMC 4-2a cell fate. Loss of *pros* produces gene expression defects in most GMCs and may be involved in establishing the GMC cell type (Doe et al., 1991; Spana and Doe, 1995); loss of *pdm-1* and *pdm-2* may affect GMC 4-2a cell division or fate (Bhat et al., 1995; Yeo et al., 1995); and loss of *ftz*, *eve*, and *hkb* all affect axon pathfinding of the RP2 neuron (Doe et al., 1988a, 1988b; this study).

Overexpression of *hkb* at stage 10, just after GMC 4-2a is born, can generate duplicate EVE-positive GMC 4-2a's and RP2 neurons. When these embryos are assayed at stage 12, 58% of the hemisegments show either three EVE-positive cells (two big and one small, consistent with a duplicate GMC 4-2a, RP2, and small RP2sib) or four EVE-positive cells (two big and two small, consistent with a normal and duplicate pair of RP2/RP2sib cells). The four-cell stage is less common, which may be due to lack of division or down-regulation of *eve* expression in the duplicate GMC 4-2a. By stage 16, only 9% of the hemisegments contain a duplicate EVE-positive "RP2" neuron, confirming that the duplicate GMC 4-2a fate is not completely stable. Interestingly, an "unstable" duplication of GMC 4-2a fate

is also produced by overexpression of *pdm-2* (Yang et al., 1993).

Two interpretations of the *hkb* overexpression results seem most likely. First, *hkb* overexpression may cause a transformation within the NB 4-2 lineage such that the second progeny (GMC 4-2b) adopts the fate of GMC 4-2a (see Figure 5A). This could be due to a transformation of NB 4-2A back to the NB 4-2 fate or a transformation of GMC 4-2b into GMC 4-2a without altering NB identity. Ectopic *hkb* expression could cause this transformation by providing a level of *HKB* RNA or protein in NB 4-2A or GMC 4-2b that matches that of NB 4-2 or GMC 4-2a, respectively. It is unknown what level of HKB protein normally exists in NB 4-2A or GMC 4-2b. Alternatively, *hkb* overexpression may induce an additional round of cell division in GMC 4-2a, resulting in the duplication of GMC 4-2a and subsequently in a duplication of the RP2 and RP2sib (see Figure 5B).

It is also possible that *hkb* overexpression leads to another NB adopting the NB 4-2 fate. We think this is unlikely because we have never observed two clearly separated EVE-positive GMCs (which might be expected if these EVE-positive cells are produced from different NB lineages).

Loss of *hkb* Results in Aberrant Motoneuron Axon Pathfinding

We used the fluorescent lipophilic tracer DiI to label specifically the entire embryonic NB 4-2 lineage in both wild-type and *hkb* mutant embryos. We could identify the "NB 4-2" lineage in *hkb* embryos based on numerous criteria, including position of the clone relative to CNS landmarks, cell number, cell position, type of neurons, and initial orientation of axon projections. Although it is formally possible that the "NB 4-2" clone derives from a different NB in *hkb* embryos, the simplest and most likely interpretation is that it represents an altered NB 4-2 lineage. In the future, this question can be answered definitively by identifying the DiI-labeled NB by position in the NB array and scoring the resulting clone in the mature CNS.

Loss of *hkb* does not alter the cell type, position, or general direction of the axonal projections of the neuronal progeny of NB 4-2. However, there are consistent defects in axon pathfinding of the RP2 and CoR motoneurons. Why are only the motoneurons affected? All three motoneurons are the most dorsal cells in the clone, which may indicate that they are born early in the NB 4-2 lineage; this is true for the RP2 neuron, which is derived from the firstborn GMC 4-2a. *hkb* is expressed early in the NB 4-2 lineage (only between stage 9 and stage 11), and thus may not be expressed in the GMCs that produce interneurons. Alternatively, there may be subtle defects in the interneurons that we are unable to score. However, *hkb* function is not limited to motoneurons in all NB lineages: there are defects in interneuron axon pathfinding in the NB 1-1 and 2-2 lineages (T. Bossing et al., unpublished data), and we observe general defects in axon fasciculation within the neuropil (see Figure 6).

We believe that the DiI phenotypes are due to autonomous defects in the NB 4-2 lineage. *hkb* is only expressed in the CNS, salivary glands, and midgut anlage; it is not expressed in the lateral bodywall tissues that could serve as motoneuron pathfinding or target recognition cues (e.g., muscles, other mesoderm, glia, trachea, sensory neurons, or epidermis). However, we cannot absolutely rule out a nonautonomous contribution to the NB 4-2 phenotype either from disruptions caused by displaced yolk (due to midgut defects), or from defects in other neurons that might provide pathfinding cues for RP2 and CoR. Absolute proof of the autonomous NB 4-2 *hkb* phenotype awaits the generation of hkb^{-} CNS clones.

How might the loss of the putative nuclear zinc finger HKB protein in NBs and GMCs lead to axon pathfinding defects? One possibility is that HKB protein persists in mature neurons and directly regulates expression of genes involved in establishing growth cone guidance. A more likely possibility is that axon defects in *hkb* embryos are due to a partial alteration in GMC cell fate; this is supported by the loss of *eve* expression in GMC 4-2a. Loss of either *ftz* or *eve* gene expression in GMC 4-2a also leads to an aberrant axon projection of the RP2 neuron, but in these mutant embryos the RP2 projects contralaterally (Doe et al., 1988a, 1988b). It is unclear why loss of *eve* alone results in a contralateral RP2 projection, whereas the combined loss of *hkb* and *eve* results in a more normal ipsilateral projection. In any case, loss of *hkb*, *ftz*, or *eve* in GMC 4-2a each results in aberrant axon pathfinding of the RP2 motoneuron, probably by affecting a gene regulatory hierarchy ultimately required in neurons for normal growth cone guidance.

Experimental Procedures

Fly Strains

We used *yellow white* (*yw*), 5953 (a homozygous viable enhancer-trap line with a P element *lacZ* reporter construct inserted 7.5 kb 3' to the *hkb* gene), hkb^{62}/TM3 (a strong hypomorphic 5953 excision allele), and *hkb' e*/TM3 *Sb e ftzlacZ* (a strong hypomorphic allele bearing a small deletion within the *hkb* transcript; Brönner et al., 1994). *y w* flies containing an *hkb* cDNA under *hsp70* promoter control (*"hs-hkb"* flies; Brönner et al., 1994) were used for *hkb* overexpression.

DNA and RNA Techniques

Genomic DNA flanking the 5953 P element insertion was isolated and nonradioactively labeled with digoxygenin using the Genius Labeling kit (Boehringer Mannheim). Genomic DNA was used for chromosome in situ hybridizations according to standard methods (Ashburner, 1989). Localization of the *HKB* RNA in whole-mount embryo in situ hybridization was done according to the protocol of Skeath and Carroll, 1992, with the exception that xylene and proteinase K treatments were omitted. Probes included digoxygenin-labeled genomic DNA or a 1.7 kb *hkb* cDNA isolated from a pNB40 library (Brönner et al., 1994).

Immunostaining

Embryos were stained using standard methods (Doe, 1992). Primary antibodies included rabbit anti-EVE (1:2500; from M. Frasch), mouse anti-FTZ (1:1000; from I. Duncan), rabbit anti-PDM-1 (1:50; from S. Poole), mouse anti-PROS MR1A (1:4; Spana and Doe, 1995), rabbit anti-β-galactosidase (1:1000; Cappel), mouse anti-BP102 (1:4; from C. S. Goodman), mouse anti-FAS II (1:10; from C. S. Goodman), and mouse anti-FAS III (1:3; from C. S. Goodman). Histochemical detection of primary antibodies was done using the HRP Vectastain Elite kit (Vector) according to manufacturer's instructions. The HRP reaction was performed using DAB substrate (Pierce Chemicals). Immunofluorescent detection of primary antibodies was done using the following secondary antibodies: donkey antimouse conjugated to rhodamine

(1:200) and donkey antirabbit conjugated to fluorescein (1:200), both from Jackson Immunoresearch, Inc. For visualization, embryos were mounted in 70% glycerol with 4% n-propyl gallate (Sigma). Immunofluorescent images were collected on a Bio-Rad MRC 1000 confocal microscope.

In all experiments, *hkb*^{1} homozygous embryos were distinguished by the absence of the *ftzlacZ* expression. For detailed observation of the stage 16 CNS, ventral nerve cords of whole-mount embryos were dissected with tungsten needles and mounted in 70% glycerol.

Heat Shock Experiments

y w (wild-type) and *y w*; *hs-hkb* embryos were collected on thin molasses caps at 30 min intervals and aged for 3.5 hr at 24°C. Embryo cap collections were parafilmed and submerged in a 37°C water bath for 18 min. Prior to submersion, a portion of the collection was dechorionated, fixed, and stained with the engrailed antibody to assess the developmental stage at time of heat shock. After heat shock, experimental embryo collections were allowed to continue development at 24°C until stage 11, stage 12, or stage 16. The embryos were then fixed and stained with an antibody to EVE.

DiI Lineage Tracing

y w (wild-type) and *hkb*^{1} *e*/TM3 *Sb e ftzlacZ* embryos were collected in 1 hr intervals and aged for 2 hr at 25°C. Single neuroectodermal cells at stage 7 were labeled with DiI as previously described (Bossing and Technau, 1994). Cells 6–8 cell diameters from the midline were targeted to increase the odds of labeling the intermediate column NB 4-2. As expected, the majority of labeled cells formed ventral epidermal clones, with about 30% delaminating to form an NB and its clonal progeny. Because labeling NB 4-2 is a low frequency event, we labeled individual neuroectodermal cells in multiple segments in each embryo. After 24 hr at 16°C, embryos containing motoneuronal projections were filleted to reveal the CNS (Thomas et al., 1984) and examined on a Bio-Rad MRC 1000 confocal microscope. Nomarski and DiI images were collected at matched 0.8 μm intervals throughout the entire CNS. DiI images were projected to show the entire clone; overlaying the projected DiI image with individual Nomarski images allowed registration of the clone with landmarks such as commissures, connectives, and identified muscles. Following image collection, embryos were stained for β-galactosidase activity to identify the *hkb* embryos. A detailed protocol is available upon request.

Acknowledgments

We thank K. Schuske and M. P. Scott for providing the 5953 line; T. Bossing for instruction in DiI labeling; K. Troka for performing the genomic plasmid rescues; E. Christ-Harned for the chromosome in situ hybridization; and I. Duncan, M. Frasch, C. S. Goodman, N. H. Patel, and S. Poole for antibodies. We especially thank Jim Skeath and Eric Spana for comments on the manuscript. This work was supported by a Proctor and Gamble Predoctoral Fellowship (Q. C. -L.); by the Sonderforschungsbereich 271 of the Deutsche Forschungsgemeinschaft (H. J.); and by the National Institutes of Health (HD 27056), the National Science Foundation (Presidential Young Investigator), and the Human Frontier Science Program (C. Q. D.). C. Q. D. is an assistant investigator of the Howard Hughes Medical Institute.

The costs of publication of this article were defrayed in part by the payment of page charges. This article must therefore be hereby marked *"advertisement"* in accordance with 18 USC Section 1734 solely to indicate this fact.

Received July 13, 1995; revised August 15, 1995.

References

Ashburner, M. (1989). Drosophila: A Laboratory Handbook and Manual (Cold Spring Harbor, NY: Cold Spring Harbor Laboratory Press).

Bhat, K.M., and Schedl, P. (1994). The Drosophila *miti-mere* gene, a member of the POU family, is required for the specification of the RP2/sibling lineage during neurogenesis. Development *120*, 1483–1501.

Bhat, K.M., Poole, S.J., and Schedl, P. (1995). *miti-mere* and *pdm-1* genes collaborate during the specification of the RP2/sib lineage in Drosophila neurogenesis. Mol. Cell Biol. *15*, 4052–4063.

Bossing, T., and Technau, G.M. (1994). The fate of the CNS midline progenitors in Drosophila as revealed by a new method for single cell labeling. Development *120*, 1895–1906.

Broadus, J., Skeath, J.B., Spana, E., Bossing, T., Technau, G., and Doe, C.Q. (1995). New neuroblast markers and the origin of the aCC/pCC neurons in the Drosophila CNS. Mech. Dev. *54*, 1–10.

Brönner, G., and Jäckle, H. (1991). Control and function of terminal gap gene activity in the posterior pole region of the Drosophila embryo. Mech. Dev. *35*, 205–211.

Brönner, G., Chu-LaGraff, Q., Doe, C.Q., Cohen, B., Weigel, D., Taubert, H., and Jäckle, H. (1994). Sp1/Egr-like zinc-finger protein required for endoderm specification and germ-layer formation in Drosophila. Nature *369*, 664–668.

Campos-Ortega, J.A. (1993). Embryonic development of the Drosophila central nervous system. In The Development of *Drosophila melanogaster*, M. Bate and A. Martinez-Arias, eds. (Plainview, NY: Cold Spring Harbor Laboratory Press), pp. 1131–1206.

Campos-Ortega, J.A., and Hartenstein, V. (1985). The Embryonic Development of *Drosophila melanogaster* (Berlin: Springer-Verlag).

Chu-LaGraff, Q., and Doe, C.Q. (1993). Neuroblast specification and formation regulated by *wingless* in the Drosophila CNS. Science *261*, 1594–1597.

Crossley, C.A. (1978). The morphology and development of the Drosophila muscular system. In The Genetics and Biology of Drosophila, Volume 2b, M. Ashburner and T.R.F. Wright, eds. (New York: Academic Press), pp. 499–560.

Doe, C.Q. (1992). Molecular markers for identified neuroblasts and ganglion mother cells in the Drosophila central nervous system. Development *116*, 855–863.

Doe, C.Q., Hiromi, Y., Gehring, W., and Goodman, C.S. (1988a). Expression and function of the segmentation gene *fushi tarazu* during Drosophila neurogenesis. Science *239*, 170–175.

Doe, C.Q., Smouse, D., and Goodman, C.S. (1988b). Control of neuronal fate by the Drosophila segmentation gene *even-skipped*. Nature *333*, 376–378.

Doe, C.Q., Chu-LaGraff, Q., Wright, D.M., and Scott, M.P. (1991). The *prospero* gene specifies cell fates in the Drosophila central nervous system. Cell *65*, 451–464.

Duffy, J.B., Kania, M., and Gergen, J.P. (1991). Expression and function of the Drosophila gene *runt* in the early stages of neural development. Development *113*, 1223–1230.

Fujita, S.C., Zipursky, S.L., Benzer, S., Ferrus, A., and Shotwell, S.L. (1982). Monoclonal antibodies against the Drosophila nervous system. Proc. Natl. Acad. Sci. USA *79*, 7929–7933.

Goodman, C.S., Bastiani, M.J., Doe, C.Q., du Lac, S., Helfand, S.L., Kuwada, J.Y., and Thomas, J.B. (1984). Cell recognition during neuronal development. Science *225*, 1271–1279.

Grenningloh, G., Rehm, E.J., and Goodman, C.S. (1991). Genetic analysis of growth cone guidance in Drosophila: Fasciclin II functions as a neuronal recognition molecule. Cell *67*, 45–57.

Patel, N.H., Snow, P.M., and Goodman, C.S. (1987). Characterization and cloning of fasciclin III: a glycoprotein expressed on a subset of neurons and axon pathways in Drosophila. Cell *48*, 975–988.

Reuter, R., and Leptin, M. (1994). Interacting functions of *snail*, *twist* and *huckebein* during the early development of germ layers in Drosophila. Development *120*, 1137–1150.

Seeger, M., Tear, G., Ferres-Marco, D., and Goodman, C.S. (1993). Mutations affecting growth cone guidance in Drosophila: genes necessary for guidance toward or away from the midline. Neuron *10*, 409–426.

Sink, H., and Whitington, P. (1990). Location and connectivity of abdominal motoneurons in the embryo and larva of *Drosophila melanogaster*. J. Neurobiol. *12*, 298–311.

Skeath, J.B., and Carroll, S.B. (1992). Regulation of proneural gene expression and cell fate during neuroblast segregation in the Drosophila embryo. Development *114*, 939–946.

Skeath, J.B., Zhang, Y., Holmgren, R., Carroll, S., and Doe, C.Q.

(1995). Specification of neuroblast identity in the Drosophila embryonic central nervous system by the *gooseberry-distal* gene. Nature *346*, 427–430.

Spana, E., and Doe, C.Q. (1995). The prospero transcription factor is asymmetrically localized to the cell cortex during neuroblast mitosis in Drosophila. Development *121*, 3187–3195.

Thomas, J.B., Bastiani, M.J., Bate, M., and Goodman, C.S. (1984). From grasshopper to Drosophila: a common plan for neuronal development. Nature *310*, 203–207.

Van Vactor, D., Sink, H., Fambrough, D.M., Tsoo, R., and Goodman, C.S. (1993). Genes that control neuromuscular specificity in Drosophila. Cell *73*, 1137–1153.

Yang, X., Yeo, S., Dick, T., and Chia, W. (1993). The role of a Drosophila POU homeodomain gene in the specification of neural precursor identity in the developing embryonic central nervous system. Genes Dev. *7*, 504–516.

Yeo, S., Lloyd, A., Kozak, K., Dinh, A., Dick, T., Yang, X., Sakonju, S., and Chia, W. (1995). On the functional overlap between two Drosophila POU homeodomain genes and the cell fate specification of a CNS neural precursor. Genes Dev. *9*, 1223–1236.

Zhang, Y., Ungar, A., Fresquez, C., and Holmgren, R. (1994). Ectopic expression of either the Drosophila *gooseberry-distal* or *proximal* gene causes alterations of cell fate in the epidermis and central nervous system. Development *120*, 1151–1161.